DALTON PERSPECTIVE

Network self-assembly patterns in Main Group metal chalcogenide-based materials

William S. Sheldrick

Lehrstuhl für Analytische Chemie, Ruhr-Universität Bochum, D-44780 Bochum, Germany. E-mail: shel@anachem.ruhr-uni-bochum.de

Received 11th May 2000, Accepted 7th July 2000
Published on the Web 23rd August 2000

Technological interest in the design of multifunctional microporous materials has stimulated recent research into the development of mild solventothermal techniques for the construction of lamellar and framework Main Group chalcogenidometalates. Reaction pathways from elemental or metal chalcogenide sources can be influenced by a variety of often interdependent factors of which counter cation size and charge, solvent polarity, pH and temperature are of paramount importance. As reviewed in this article, the presence of predominant solution species such as cyclic tripyramidal $M_3S_6^{3-}$ (M = As or Sb) or edge-bridged ditetrahedral $Sn_2E_6^{4-}$ anions (E = S or Se) as molecular building units and their participation in columnar substructures is characteristic for M_2S_3- and SnE_2-based anionic networks. Hierarchical topological relationships between individual members of structural families of the type $A_xM_yE_z$ (A = alkali metal or alkylammonium cation) can be established that provide a detailed insight into probable multiple-step cation-directed self-assembly mechanisms. These findings enable the development of rational guidelines for the employment of suitable counter cations in controlling the condensation of small solution species into chains, sheets or frameworks, whose cavities reflect the spatial requirements of the structure-directing agent.

1 Introduction

Recent increased interest in Main Group chalcogenidometalates has primarily been motivated by their apparent technological potential as multifunctional materials capable of combining the ion-exchanging and catalytic features of microporous solids[1,2] with the semiconducting properties of metal sulfides or selenides. Perceived areas of application have ranged from lamellar alkylammonium thiostannates(IV) as molecule discriminating sensors[3,4] to tellurium-rich alkali metal tellurides as promising materials in the search for low-dimensional metals.[5] In an extension of the traditional soft hydrothermal techniques employed for the synthesis of molecular sieves[6] a variety of polar fluids (*e.g.* water, CH_3OH, en, CH_3CN) have been shown to be suitable as solventothermal reaction media[7,8] for the self-assembly of metal chalcogenide-based anionic networks. The relatively high polarity of methanol, coupled with its low viscosity and reduced tendency to cocrystallise in comparison to water, have led to increased interest in the use of this solvent in the temperature range 110–200 °C, particularly for the preparation of selenido- and tellurido-metalates.[7] Recent work by Li, Proserpio and co-workers[8] has also underlined the potential of superheated ethylenediamine as an alternative reaction medium for this purpose.

Despite significant advances in the past decade, the development of a rational approach to the synthesis of tailored zeolites and molecular sieves still remains a major challenge.[6,9] Although this is certainly also the case for metal chalcogenide-based materials, the recurrent presence of dominant solution species such as cyclic $As_3S_6^{3-}$, adamantane-like $Ge_4E_{10}^{4-}$ or edge-bridged ditetrahedral $Sn_2E_6^{4-}$ (E = S or Se) entities in the role of molecular building blocks within the anionic networks of ternary phases $A_xM_yE_z$ (A = alkali metal or alkylammonium cation; M = Group 14/15 metal) has nurtured speculation on possible guidable self-assembly pathways. Solventothermal reaction mechanisms can, of course, be affected by a variety of factors of which counter cation size, shape and charge, solvent polarity and pH, temperature and reaction time are often of paramount importance.[7] Changing any one of these parameters may have an effect on several others, so careful control of reaction conditions is a prerequisite to any attempt to evaluate the influence of individual variables on the resulting network topology.

Before turning in detail to mechanistic aspects of Main Group chalcogenidometalate construction it is instructive briefly to consider the results of research carried out on the direction and kinetics of zeolite and molecular sieve synthesis. There is now a considerable body of experimental evidence that the small silicate anions observed by vibrational spectroscopy and NMR in hydrothermal reaction solutions merely adopt a spectator role and do not themselves self-assemble to generate a resulting zeolite framework.[6,10] Davis and Lobo[6] have suggested that individual solution species are not directly incorporated into a growing crystal but rather condense to extended columnar or lamellar substructures that cannot be detected by short range spectroscopic techniques. Such extended entities with medium-range order are present in nucleation centres and

William S. Sheldrick was born in 1945 in Huddersfield, UK, and studied chemistry at the University of Cambridge, where he received his Ph.D. in 1969. After a period of two years with an Alexander von Humboldt Fellowship at the Technical University of Braunschweig, he took up a position at the Gesellschaft für Biotechnologische Forschung in 1973. He completed his Habilitation in 1976 and moved to the University of Kaiserslautern in 1983. The appointment to his present Full Professorship at the Ruhr University of Bochum followed in 1989. His research interests, as documented in more than 400 publications, include analytical aspects of biocoordination chemistry and the solid state chemistry of heavier Group 14–16 elements.

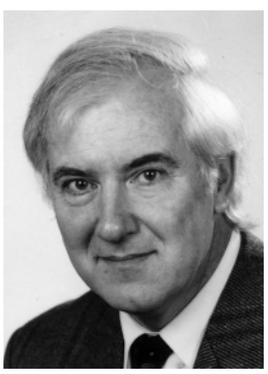

William S. Sheldrick

DOI: 10.1039/b003762l

participate in the subsequent generation of the long-range structure of a material, whether this be through solution transport or solid hydrogel reorganisation, or a combination of both. Davis and Lobo also rationalised the influence of hydrated alkali metal or organic cations on the ultimate zeolite framework by concluding that these are capable of functioning in three distinct ways, namely (i) in a space-filling manner, (ii) as structure directing agents and much more rarely (iii) as true templates.[6] According to this definition the term "templating" should only be used to describe a process during either gelation or nucleation in which a specific cation organises the condensation of oxide co-ordination tetrahedra around itself into a particular topological arrangement. Such characteristic units, whose geometrical structure reflects the size, shape and charge of the templating cation, then self-assemble as initial building blocks into a unique polymeric network. In contrast, the term "structure direction" in the above sense refers to a less specific process in which a restricted number of cations of identical charge and relatively similar size can influence network construction, in combination with other factors such as pH or temperature, so as to generate a particular anionic structure.

Despite recent advances in multitechnique *in situ* experiments, that can span the full range of atomic length scales during the formation of microporous solids under hydrothermal or solventothermal conditions,[9] most evidence for possible self-assembly mechanisms is still currently provided by careful variation of the parameters controlling the structure direction of topologically related networks. For instance, on the basis of such information, Ozin and co-workers[11,12] have recently proposed a model for the formation of aluminophosphates in which sheets and three-dimensional frameworks are generated by hydrolysis and condensation of an initial chain structure.

My co-workers and I have carried out a detailed study of the structure-directing influence of cation size, solvent polarity, pH and temperature on the construction of novel Main Group metal chalcogenide-based materials. In particular, our recent work has allowed us to establish families of structurally related thioarsenate(III) and selenidostannate(IV) networks with increasing degrees of anion condensation, whose connectivity patterns provide insight into probable self-assembly pathways. These results will therefore be highlighted in the present article, which considers the role of templates or structure-directing agents in organising the condensation of dominant solution species such as Te_y^{2-} chains, $[As_3S_6]^{3-}$ ring anions or ditetrahedral $[Sn_2E_6]^{4-}$ species (E = S or Se) during the solventothermal synthesis of polymeric chalcogenidometalates. For a detailed discussion of solventothermal techniques or for a comprehensive report on the structural chemistry of chalcogenidometalates of the heavier Group 14 and 15 elements (up to 1998) the reader is referred to our recent review articles[7,13] on these topics.

2 Co-ordination polyhedra and connectivity

A variety of novel polychalcogenidometalates of the heavier Group 14/15 elements have been prepared in recent years both in molten alkali metal polychalcogenide fluxes[14,15] at 200–600 °C and by employing elemental Se or Te as starting components for reactions carried out under mild solventothermal conditions. Although many of these materials contain simple E_z^{2-} chains, the characteristic propensity of tellurium to adopt hypervalent co-ordination polyhedra also leads to the presence of T-shaped $TeTe_3$ and square-planar $TeTe_4$ units in polytellurides and extended telluridometalates. This observation poses the mechanistic question as to how and when such building blocks are formed during the construction of tellurium-rich networks, a topic that will be considered in Section 4. Selenium, in contrast to its heavier congener, is far less inclined to exhibit co-ordination numbers higher than two. However, as for discrete oligotellurides of higher nuclearity, cyclisation is

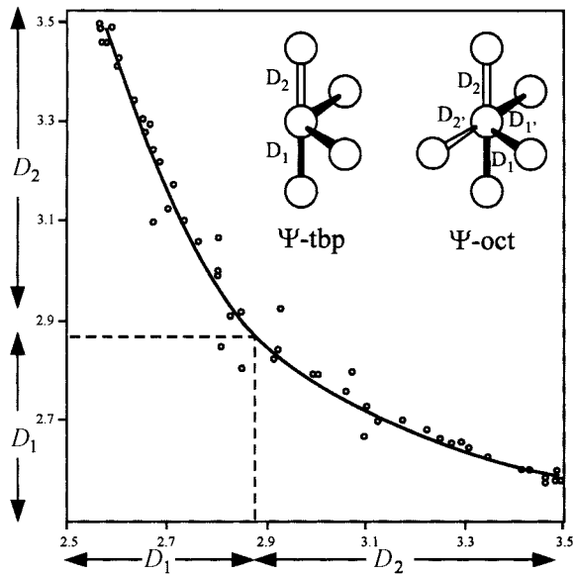

Fig. 1 Structural correlation of *trans*-related Sb–Se distances D_1 and D_2 in the ψ-$SbSe_4$ trigonal bipyramids and ψ-$SbSe_5$ octahedra of Sb_2Se_3[20] and the selenidoantimonates(III) $KSbSe_2$, $RbSb_3Se_5$, $BaSb_2Se_4$ and $Cs_2Sb_4Se_8$.[21–24]

also characteristic for oligoselenides Se_y^{2-} with $y > 9$, leading, for instance, to the presence of two T-shaped $SeSe_3$ units in the fused Se_6 rings of $(Ph_3PNPPh_3)_2Se_{10}\cdot DMF$[16] or a square-planar central $SeSe_4$ unit in the bicyclic Se_{11}^{2-} anion of $(Ph_4P)_2Se_{11}$.[17,18]

Oligomeric or polymeric chalcogenidometalates containing ME_4 tetrahedra (E = S, Se or Te) with the group oxidation state (+v) are unknown for the heavier members (M = As, Sb or Bi) of Group 15. Like its neighbour selenium, a reluctancy to extend its co-ordination number beyond the formal valency value is also apparent for As^{III}, for which relatively undistorted ψ-AsE_4 trigonal bipyramids have only been reported[19] for the $^1_\infty[As_6S_{10}]^{2-}$ double chains in $(Me_4N)_2As_6S_{10}$. In this and other relevant co-ordination polyhedra of trivalent Group 15 elements (*i.e.* ψ-ME_3 tetrahedra and ψ-ME_5 octahedra) use of the Greek letter ψ implies that one site is formally occupied by a non-bonded electron pair. The effective restriction in the participating co-ordination polyhedra for As^{III} to ψ-AsE_3 tetrahedra leads to a striking paucity in the number of structural types adopted by thio- and selenido-arsenates(III) in comparison to Sb_2E_3-based materials (E = S or Se). The characteristic ability of Sb^{III} to extend its co-ordination number beyond three in its chalcogenidometalates leads to the frequent observation of ψ-SbE_4 trigonal bipyramids and occasionally ψ-SbE_5 octahedra. However, the assignment of a particular co-ordination polyhedron often remains a somewhat arbitrary undertaking, owing to the fact that many of the participating approximately linear E–Sb–E three-centre bonds are strongly asymmetric. As illustrated by the structural correlation of *trans*-sited Sb–Se bond distances presented for Sb_2Se_3[20] and selected selenidoantimonates(III)[21–24] in Fig. 1, differences for $\Delta = D_2 - D_1$ of 0.35 Å or greater are typical for the inner co-ordination sphere of the Group 15 element. According to the widely used bond-valence concept, first introduced by Pauling[25] and more recently improved and extended by Brown[26] and O'Keeffe and co-workers,[27] individual bond valences s_{ij} to atoms j in the environment of an atom i of valency V_i ($V_i = \Sigma_j s_{ij}$) can often be satisfactorily estimated in inorganic crystal structures by employing expressions of the type $s_{ij} = \exp[(D_0 - D_{ij})/B]$ where B is invariant and approximately 0.37 Å,[28] D_0 represents a bond length of unit variance and D_{ij} the distance between the participating atoms. This approach is also suitable for thio- and selenido-antimonates(III) (Fig. 1), as indicated by the limited degree of scattering for their opposite D_1/D_2 values from the idealised exponential correlation functions. The

observed wide spread of *trans*-sited Sb–E distances depicted in Fig. 1 for Sb_2Se_3-based materials and also found in the thioantimonates(III)[29,30] indicates that the energy hypersurface for E–Sb···E interactions must be rather flat. This means, of course, that the degree of asymmetry for such three-centre bonds in a particular chalcogenidoantimonate(III) will strongly be influenced by interactions between its anionic network and the charge-balancing counter cations.

Although there is some confusion in the literature it is reasonable to assign[13] the dimensionality of Sb_2E_3-based materials by including both short (D_1) and intermediate Sb–E interactions (*e.g.* D_2 for $D_2 - D_1 < 0.45$ Å). An instructive example for this procedure is provided by $RbSb_3Se_5$, which exhibits short (2.535–2.729 Å), intermediate (3.055–3.103 Å) and long (3.346–3.488 Å) Sb–Se distances.[22] When only the first category of bonds is considered, then isolated fused tricyclic $[Sb_6Se_{10}]^{2-}$ anions are present, that are constructed from corner-bridged ψ-$SbSe_3$ tetrahedra. Inclusion of the intermediate secondary bonds leads, in contrast, to the more suitable description of the anionic substructure of $RbSb_3Se_5$ as polymeric $^2_\infty[Sb_3Se_5]^-$ sheets, containing ψ-$SbSe_3$ tetrahedra and ψ-$SbSe_4$ trigonal bipyramids in a 1:2 relationship. If the very weak interactions in the range 3.346–3.488 Å are also taken into account, then it is possible to classify $RbSb_3Se_5$ as a framework selenidoantimonate(III). Similar considerations apply to the heavier Group 15 homologue Bi^{III}, whose propensity to adopt higher co-ordination numbers, including 6, is more pronounced than for Sb^{III}. Edge bridging of distorted BiE_6 octahedra (E = Se or Te) leads to the regular occurrence of chains and sheets (*e.g.* $Cs_3Bi_7Se_{12}$[31] and $SrBiTe_3$[32]), that can be regarded as fragments of an NaCl-type lattice.

With few exceptions[13] polymeric networks have only been characterised for heavier Group 14 chalcogenidometalate anions with M (Ge or Sn) in its highest oxidation state (+IV). The absence of both binary chalcogenides PbE_2 (E = S, Se or Te) and chalcogenidoplumbates(IV) is in accordance with the decrease in stability of the +IV state on going down the Group. GeE_2-based materials contain exclusively GeE_4 tetrahedra as molecular building blocks, and this restriction to only one co-ordination polyhedron taken together with the endemic formation of adamantane-like units $[Ge_4E_{10}]^{4-}$ leads, in analogy to the behaviour of neighbouring As^{III}, to a paucity in the number of structural types exhibited by chalcogenidogermanates(IV). In contrast, Sn^{IV} is able to extend its co-ordination number from 4 in the dominating ditetrahedral solution species $[Sn_2E_6]^{4-}$ to 5 (trigonal bipyramidal) or 6 (octahedral) in its polymeric SnE_2-based anionic networks. However, it is important to register an apparent dependency on the electronegativity and size of the chalcogen partner in this context. The highest known co-ordination numbers in structurally characterised chalcogenidostannates(IV) are 6 for E = S (*e.g.* SnS_6 octahedra in $Rb_2Sn_3S_7{\cdot}2H_2O$[33] and $Cs_4Sn_5S_{12}{\cdot}2H_2O$[34]), 5 for E = Se (*e.g.* $SnSe_5$ trigonal bipyramids in $Rb_2Sn_4Se_9{\cdot}H_2O$[35] and $Cs_2Sn_3Se_7$[36]) and only the valency value of 4 for E = Te (*e.g.* $SnTe_4$ tetrahedra in $Rb_4Sn_4Te_{17}$[5] and Cs_2SnTe_4[37]).

In contrast to the oxide-based silicates,[38] both corner-(M–E–M) and edge-bridging (M-(μ-E)$_2$-M) connectivities are possible for ME_z polyhedra in the chalcogen-containing anions of the heavier Group 14/15 elements. The ability of Group 14 ME_4 tetrahedra (M = Ge or Sn) to exhibit edge bridging reflects the essentially p character of the M–E bond, that facilitates the adoption of endocyclic E–M–E and M–E–M angles close to 90° in four-membered $(ME)_2$ rings. Effectively no distortion is required to provide such an angle, when the bridging chalcogen atoms E are sited axial (ax) to one M atom and equatorial (eq) to the second M atom in an SnE_5 trigonal bipyramid or a ψ-ME_4 trigonal bipyramid (M = Sb or Bi). Edge bridging is indeed characteristic for these co-ordination polyhedra and its adoption by both E_{ax}/E_{eq} pairs in SnE_5 trigonal bipyramids (E = S or Se) results in the frequent observation of $^1_\infty[SnE_3]^{2-}$ chains as a structural component of lamellar or framework thio- and selenido-stannates(IV).[13,39] In contrast to oxide-based silicates, where the soft bending potential[38,40] for Si–O–Si linkages favours the adoption of wide angles between 120 and 180°, a much narrower typical range (90–115°) is also observed for M–E–M (E = S or Se) bridges between ME_z co-ordination polyhedra with shared corners.

3 Structure direction

As discussed in Section 1, although counter cation size, shape and charge play a central role during the construction of metal chalcogenide-based networks, one particular anionic substructure may often be generated in the presence of different structure-directing agents. Before considering individual classes of compounds in more detail, it is, therefore, necessary to identify those characteristic structural parameters that should reflect the general structure-directing influence of cation size and charge on the topology of resulting chalcogenidometalate networks.

3.1 Anion condensation grade (*c*)

A general trend towards higher condensation grades c ($c = y/z$) is apparent for the anions $[M_yE_z]^{m-}$ of Group 14/15 chalcogenidometalates $A_xM_yE_z$ or $B_xM_yE_z$ as the size of their alkali metal A ($m = x$) or alkaline earth cation B ($m = 2x$) increases. Respective c values can lie in the ranges $0.25 < c < 0.50$ (Group 14) and $0.333 < c < 0.667$ (Group 15) for oligonuclear or polymeric anions in these metal chalcogenide-based materials. As the number of potentially available chalcogen co-ordination partners p per unit of anion charge ($p = z/m$) will increase with parameter c, larger Group 1/2 counter cations will exhibit a general structure-directing influence that favours higher degrees of anion condensation. For instance, $K_4Sn_3Se_8$ ($c = 0.375$),[41] $Rb_2Sn_2Se_5$ ($c = 0.40$)[42] and $Cs_2Sn_3Se_7$ ($c = 0.429$)[36] can be synthesized under similar methanolothermal conditions. Likewise anion condensation grades greater than 0.60 have only been reported in solvent-free alkali metal chalcogenidoantimonates(III) with the large Cs^+ counter cation, *e.g.* $Cs_2Sb_8S_{13}$ ($c = 0.615$)[43] and $Cs_4Sb_{14}S_{23}$ ($c = 0.609$).[44] The highest known values of c for the smaller Rb^+ and K^+ cations have been observed in $RbSb_3Se_5$ ($c = 0.600$)[22] and $K_2Sb_4S_7$ ($c = 0.571$).[45] Lowering the pH value of a hydrothermal reaction system will, of course, also favour an increased degree of anion condensation and any resulting incommensurability between the size of anion voids and the charge-compensating counter cations can often be compensated for by the incorporation of solvent molecules into the resulting solid state structure.

3.2 Dimensionality (*d*)

For Group 14/15 chalcogenide-based materials $A_xM_yE_z$, simple packing considerations suggest that lowering the dimensionality d of a polymeric anionic network should, in general, enable the achievement of a higher degree of space filling for larger cations. Whereas the smaller alkali metal cations Na^+ and K^+ should be capable of directing the self-assembly of 3-D anionic frameworks, more voluminous cations such as Cs^+ or R_4N^+ (R = Me, Et or *n*Pr) would be expected to stabilise sheets or chains. No less than 10 thioantimonates(III) of the formula types $A_2Sb_4S_7$ and BSb_4S_7 have been structurally characterised and, as listed in Table 1, a general correlation between their dimensionality and cation size is clearly apparent. For instance, a 3-D framework anion has only been assembled in the presence of the relatively small K^+ cation. In contrast, employment of large cations such as Cs^+, $[H_2pip]^{2+}$ or $[Mn(en)_3]^{2+}$ leads to the construction of infinite chains $^1_\infty[Sb_4S_7]^{2-}$.

3.3 Average M co-ordination numbers (*n*)

Anionic networks containing corner-bridged Group 14 ME_4

Table 1 Dimensionality (*d*) and co-ordination numbers (CN) of the pnictogen (M = As or Sb) and sulfur atoms in thio-arsenates(III) and -antimonates(III) of the formula type $^{d}_{\infty}[M_4S_7]^{2-}$

		No. of M with		No. of S with			
Compound	*d*	CN = 3	CN = 4	CN = 1	CN = 2	CN = 3	Ref.
$K_2Sb_4S_7$	3	2	2	0	7	0	45
$(C_2H_5NH_3)_2Sb_4S_7$	2	3	1	1	6	0	46
$K_2Sb_4S_7{\cdot}H_2O$	2	2	2	0	7	0	47
$Rb_2Sb_4S_7{\cdot}H_2O$	2	2	2	0	7	0	48
$Rb_2Sb_4S_7$	2	0	4	0	6	1	49
$(Me_4N)_2As_4S_7$	1	4	0	2	5	0	19
$(NH_4)_2Sb_4S_7$	1	4	0	2	5	0	50
$(H_2pip)Sb_4S_7$	1	4	0	2	5	0	51
$[Mn(en)_3][Sb_4S_7]$	1	4	0	2	5	0	52
$Cs_2Sb_4S_7$	1	3	1	1	6	0	53
$SrSb_4S_7{\cdot}6H_2O$	1	3	1	1	6	0	54

pip = Piperidine.

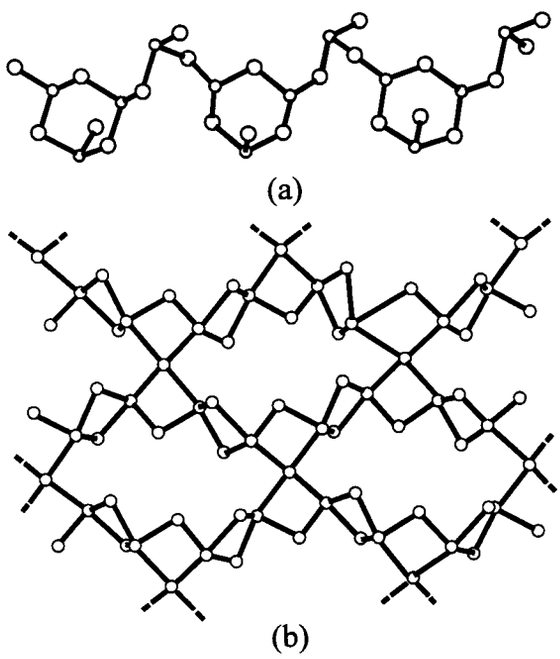

Fig. 2 (a) The $^{1}_{\infty}[As_4S_7]^{2-}$ *zweier* single chains of $(Me_4N)_2As_4S_7$ [19] with $n = 3.0$ and (b) the $^{2}_{\infty}[Sb_4S_7]^{2-}$ sheets of $Rb_2Sb_4S_7$ [49] with $n = 4.0$.

tetrahedra will be more flexible in a conformational sense than those based on edge-bridged ME_5 trigonal bipyramids or ME_6 octahedra. Similar considerations apply to ψ-ME_3 tetrahedra in comparison to ψ-ME_4 trigonal bipyramids or ψ-ME_5 octahedra of Group 15 elements. As flexible anionic networks should favour higher co-ordination numbers and denser structures for voluminous cations, a trend towards lower average M co-ordination numbers (*n*) might be expected as the cation size increases for chalcogenidometalates of a given formula type. This is indeed the case for the thioantimonates(III) $^{d}_{\infty}[Sb_4S_7]^{2-}$ presented in Table 1. With the exception of the lamellar network of $(C_2H_5NH_3)_2Sb_4S_7$ ($n = 3.25$), *n* is smaller in chain anions ($n = 3.0$, 3.25) than in sheet or framework anions ($n = 3.50$, 4.00). A comparison of the strikingly different connectivity patterns in the chains of $(Me_4N)_2As_4S_7$ ($n = 3.0$) and the 2-D anionic network of $Rb_2Sb_4S_7$ ($n = 4.0$) is provided in Fig. 2. The characteristic cyclic $[M_3S_6]^{3-}$ building units of the former compound are also present in the analogous polyanions of the thioantimonates(III), $(NH_4)_2Sb_4S_7$, $(H_2pip)Sb_4S_7$ and $[Mn(en)_3][Sb_4S_7]$.

4 Alkali metal cation templation of polytelluride nets

According to the Zintl–Klemm concept, the valence electrons of the alkali metal atoms A in tellurium-rich tellurides A_xTe_y can be regarded as being effectively fully transferred to the anionic substructure of the more electronegative partner Te. The striking variety of known formula types ($x/y = 5/3$, 2/1, 1/1, 2/3, 2/5, 1/3, 1/4, 1/6, 2/13, 1/7 and 3/22) and structural motifs for this class of compounds reflect the propensity of tellurium both to catenate and to participate in hypervalent co-ordination polyhedra. Whereas discrete anions are observed for $x/y \geq 2/3$, polymeric chain and lamellar anionic networks are present in such tellurides when $x/y \leq 2/5$.[55]

The very tellurium-rich alkali metal polytellurides Cs_3Te_{22} [56] and $RbTe_6$,[57] whose component lamellar nets $^{2}_{\infty}[Te_6]^{3-}$ and $^{2}_{\infty}[Te_6]^{-}$ are depicted in Fig. 3(a) and 3(b), can be isolated under soft methanolothermal reaction conditions. For instance, the reaction of Cs_2CO_3 with As_2Te_3 in superheated methanol at 195 °C leads to the construction of the unique crystal lattice of Cs_3Te_{22}, in which the planar thinned 4^4 nets $^{2}_{\infty}[Te_6]^{3-}$ with their Te_4 and Te_{12} squares are separated by crown-shaped Te_8 rings (Fig. 4). These contrasting substructures are stabilised by the presence of Cs^+ counter cations at the centres of the Te_{12} squares and may themselves be regarded as reflecting the non-metallic and metallic sides of tellurium chemistry.

Spectroscopic speciation studies [58–61] on alkali metal tellurides in ethylenediamine or liquid NH_3 solution have confirmed the presence of short oligotelluride chains Te_y^{2-} ($y = 2$ or 3) but provided no evidence for neutral cyclic species Te_y or anions with $y > 4$. It is, therefore, reasonable to assume that the strikingly different tellurium substructures in Cs_3Te_{22} must reflect a specific templating role of the alkali metal cation during a multiple-step reaction pathway. This presumption led my group to carry out a systematic investigation of the methanolothermal reaction of Cs_2CO_3 with As_2Te_3 at temperature intervals of 5 °C within the range 145–195 °C in the hope of gaining insight into the mechanism of formation of Cs_3Te_{22}. Interestingly, a unique telluridoarsenate(II) $Cs_4As_2Te_6$ with centrosymmetric isolated $As_2Te_6^{4-}$ anions [62] may be isolated from a superheated methanol solution at 145 °C. However, on raising the temperature by a mere 15 °C only the caesium tellurides Cs_2Te_5 and Cs_2Te_{13} can be obtained as crystalline products.[63] On ignoring secondary Te1 · · · Te3 interactions of 3.181(2) and 3.261(2) Å, Cs_2Te_{13} contains Te_{13}^{2-} chains, that are clearly stabilised by templating Cs^+ cations (Fig. 5). The bond lengths (2.755(2)–2.808(2) Å) and angles in the central Te_7 unit are reminiscent of those of the Te_8 rings in Cs_3Te_{22} [56] and this fragment can indeed be regarded as an incomplete crown. The long Te_{13}^{2-} chains in Cs_2Te_{13} are themselves connected through weaker Te1–Te3 bonds into undulating sheets, in which the incomplete Te_7 crowns are linked by $^{1}_{\infty}[Te_6]^{2-}$ ladders of fused Te_4 rectangles and Te_6 rings.

The template-controlled formation of the separated effectively neutral Te_8 crowns and defective square planar $^{2}_{\infty}[Te_6]^{3-}$

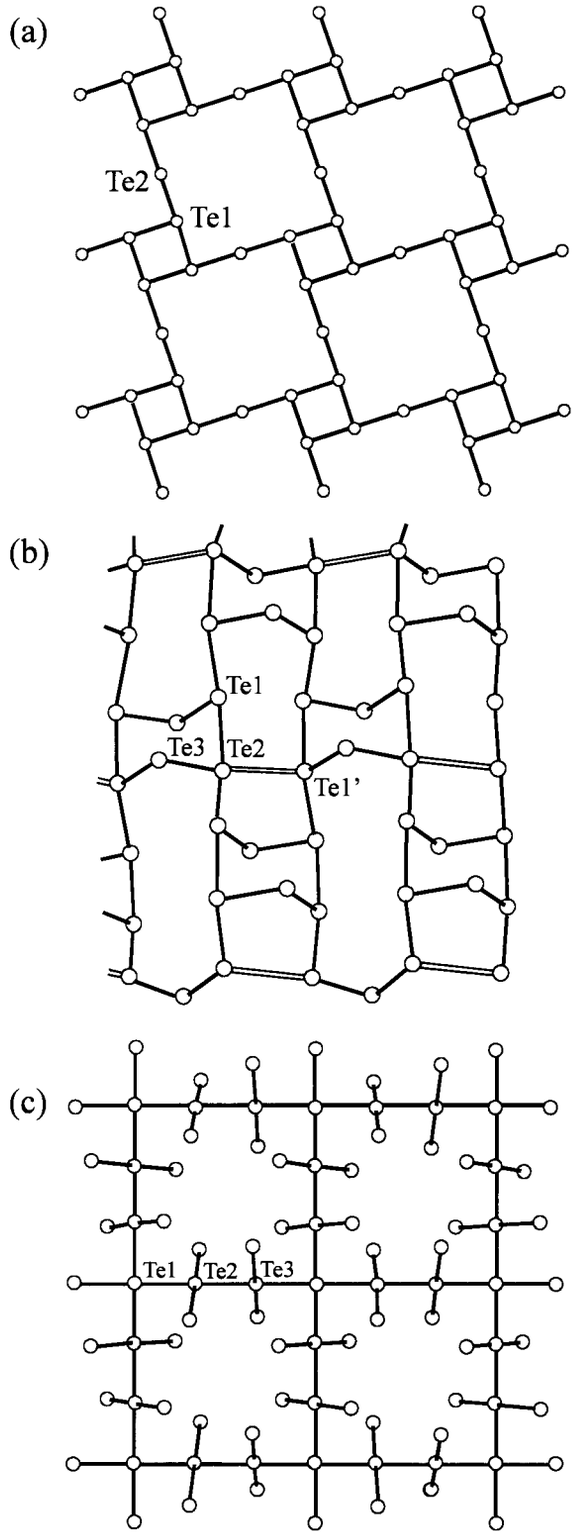

Fig. 3 Polytelluride nets: (a) $^{2}_{\infty}[Te_6]^{3-}$ in Cs_3Te_{22},[56] (b) $^{2}_{\infty}[Te_6]^{-}$ in $RbTe_6$[57] and (c) $^{2}_{\infty}[Te_5]^{4-}$ in $Rb_4Sn_4Te_{17}$[5] for which the terminal Te atoms of bridging ditetrahedral Sn_2Te_6 units are also shown. One half of the weak Te2···Te1 interactions (3.449(3) Å, open bonds) are included for $^{2}_{\infty}[Te_6]^{-}$.

telluride nets in Cs_3Te_{22} (Fig. 4) can readily be mechanistically explained on the basis of the Cs_2Te_{13} structure. Following their generation as extended solution species by Cs^+ templation, medium range Te_y^{2-} chains such as Te_{13}^{2-} participate directly in construction of the weakly bonded sheets of Cs_2Te_{13}. Cleavage of the symmetry-related Te3–Te4 bonds and addition of a Te atom to the liberated Te_7 fragment could afford the isolated crown-shaped Te_8 rings that co-ordinate the Cs^+ cations of Cs_3Te_{22}. Rearrangement of the remaining $^{1}_{\infty}[Te_6]^{2-}$ ladders into a

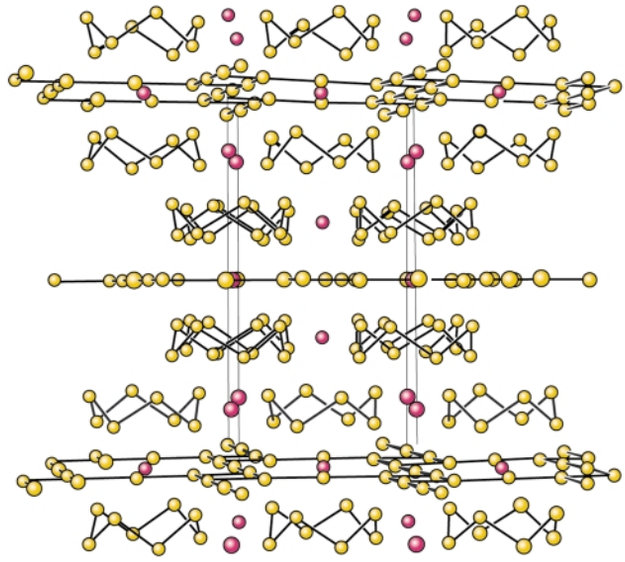

Fig. 4 The crystal structure of Cs_3Te_{22}[56] in projection perpendicular to [100].

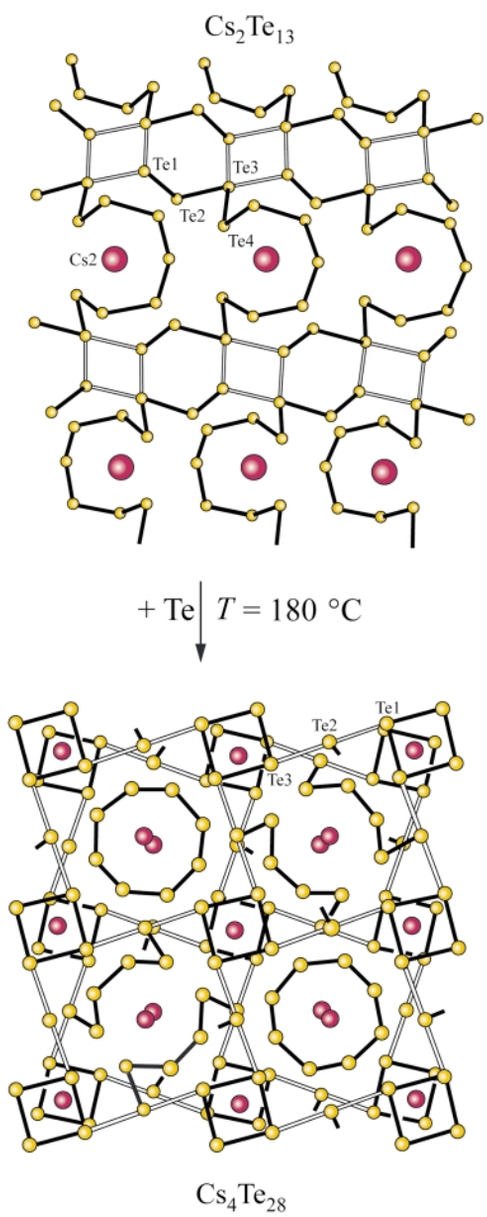

Fig. 5 The structural relationship between the metastable phases Cs_2Te_{13} and Cs_4Te_{28}[63] on the reaction pathway to Cs_3Te_{22}.[56]

thinned 4^4 net with Te_4 and Te_{12} squares can then be achieved by cleavage of the old Te1–Te2 bonds and formation of new Te1–Te2 contacts between the Te_4 rings of previously adjacent ladders. Extended Hückel calculations[64,65] on the $^2_\infty[Te_6]^{3-}$ sheets of Cs_3Te_{22} have yielded atomic charges of −1.06 for the linear tellurium atoms Te2 and −0.22 for the Te1 atoms of the four-membered rings. These findings suggest that the probably metallic $^2_\infty[\{Te_4Te_{4/2}\}]^{3-}$ layer can be described in an approximate manner as a series of Te_4^- squares [d(Te1–Te1′) = 3.003(1) Å] coupled through Te^- spacers [d(Te1–Te2) = 3.077(1) Å]. The previous discussion illustrates not only the decisive templating role of the Cs^+ cation but also the importance of Te···Te secondary interactions for the formation of the $^2_\infty[Te_{13}]^{2-}$ sheets of Cs_2Te_{13} prior to separation of the Te_8 crowns and defective square planar $^2_\infty[Te_6]^{3-}$ nets in Cs_3Te_{22}. The overlap populations of 0.016 and 0.012 for the Te1···Te3 bonds are of the same order as those reported for transition metal tellurides, where they play an important role in determining the structural and transport properties of such materials.[66]

A second intermediate metastable phase Cs_4Te_{28} (Fig. 5) can be isolated together with Cs_2Te_5 (30%) and Cs_3Te_{22} (8%) in low yield (3%) on raising the temperature of the superheated methanol to 180 °C for the reaction between Cs_2CO_3 and As_2Te_3. The possible existence of a compound of this stoichiometry (Cs_2Te_{14}) with $^2_\infty[Te_6]^{2-}$ sheets was postulated by Hoffmann and co-workers[64] on the basis of their extended Hückel calculations. Cs_4Te_{28} does, at first sight, appear to contain $^2_\infty[\{Te_4Te_4\}]^{2-}$ layers, although half of its potential Te_8 crowns are broken and the resulting fragments bonded to the planar sheets. However, if the longer Te1–Te2 (3.153(2) Å) and Te2–Te3 (3.194(2) Å) bonds are disregarded (open bonds in Fig. 5), then both Te_6^{2-} chains and isolated Te_4 squares (Te1–Te1′ distances, 2.911(2), 2.955(2) Å) can be identified as further structural entities in addition to the Te_8 rings. Although this description would appear to be appropriate, extended Hückel calculations suggest that the Te_4 rings should in fact be described as Te_4^- (charge −0.94) and the Te_6 chains as Te_6^- (charge −1.06).[5] Support for the probable intermediate role of weakly bonded $^2_\infty[Te_{13}]^{2-}$ sheets (as in Cs_2Te_{13}) and $^2_\infty[Te_{20}]^{4-}$ frameworks (as in Cs_4Te_{28}) on the methanolothermal reaction pathway of Cs_2CO_3 and As_2Te_3 to Cs_3Te_{22} is provided by the experimental observation that the latter phase is the only very tellurium-rich telluride (x/y < 1/4) that can be isolated at 195 °C following an initial tempering period at 160 °C.

The $^2_\infty[Te_6]^{2-}$ layers of $RbTe_6$ (Fig. 3b) can also be constructed in high yield (79%) under methanolothermal conditions, in this case by reaction of Rb_2CO_3 with Te in the presence of Ge (as reducing agent) at 160 °C. However, the specific templating role of the Rb^+ cations in presumably prefabricating long Te_y^{2-} chains prior to crystallisation cannot be discerned from the fused chair-shaped Te_6 and Te_{10} rings of the final $^2_\infty[Te_6]^-$ sheets (as is also the case for Cs_3Te_{22}) and attempts to isolate intermediate phases have remained unsuccessful. On ignoring the longer Te1···Te2 distances (3.195(3), 3.214(3) Å) of the T-shaped Te(1)Te_3 and Te(2)Te_3 units it is possible to recognise individual Te_3 chains (d(Te1–Te2) 2.777(3), d(Te2–Te3) 2.789(2) Å) with a formal charge of −0.5.

Band structure calculations have suggested[5,64] that the defective square-planar $^2_\infty[Te_6]^{3-}$ and $^2_\infty[Te_5]^{4-}$ nets (Fig. 3a and 3c) of respectively Cs_3Te_{22} and $Rb_4Sn_4Te_{17}$ could be low-dimensional metals. Interestingly, the latter polytelluridostannate(IV) can be isolated by performing the methanolothermal reaction of Rb_2CO_3 with Te in the presence of elemental tin instead of germanium. Te2 and Te3 atoms of its parallel $^2_\infty[Te_5]^{4-}$ sheets are linked through ditetrahedral Sn_2Te_6 spacer units to construct a unique framework structure. Comparison of the tellurium nets in $RbTe_6$ and $Rb_4Sn_4Te_{17}$ suggests that a Rb^+-directed assembly of Te sheets similar to those in the former polytelluride could well take place prior to the final assembly of $^3_\infty[Sn_4Te_{17}]^{4-}$. If this is indeed the case, then generation of the Te_{12} squares of the thinned 4^4 tellurium net of $Rb_4Sn_4Te_{17}$ can be perceived as being achieved by Te–Te bond cleavage accompanied by concomitant strengthening of one half of the weaker Te1–Te2 interactions (3.449(3) Å, depicted as open bonds in Fig. 3b). On also considering the caesium tellurides Cs_2Te_{13}, Cs_4Te_{28} and Cs_3Te_{22}, this approach indicates that mechanistic guidelines can indeed be developed that take the templating ability of the heavier alkali metal cations into account when describing the structural relationships between their tellurium-rich tellurides. This, in turn, offers some hope for a rational design of synthetic strategies for this promising class of novel materials.

5 Structure direction of thio-arsenates(III) and -antimonates(III)

Group 15 element sulfides M_2S_3 (M = As or Sb) dissolve in alkaline aqueous solution to afford ψ-tetrahedral MS_3^{3-} anions together with oxo- and oxothio-anions. UV/Vis spectroscopic and potentiometric studies[67] have demonstrated that such mononuclear AsS_3^{3-} anions readily condense to corner-bridged dipyramidal $As_2S_5^{4-}$ and cyclic tripyramidal $As_3S_6^{3-}$ anions, of which the latter predominate in acid or mildly alkaline solution (pH ≤ 11). Trinuclear anions of the latter type can be extracted from ethylenediamine (en) solution in the form of salts $[H_2en]_3[As_3S_6]_2\cdot 6en$ or $[Ba(en)_4]_3[As_3S_6]_2$, whose six-membered As_3S_3 rings exhibit chair conformations with equatorially sited terminal S atoms.[68]

As previously discussed in Section 2, the effective restriction of the participating co-ordination polyhedra to ψ-AsS_3 tetrahedra leads to a paucity of potential structure types for the ternary thioarsenates(III). On assuming constancy of both n (n = 3) and the dimensionality d (d = 1) for this class of materials, initial condensation of the predominant solution species $As_3S_6^{3-}$ and $[As_ySy_{2y+1}]^{(y+2)-}$ (y = 1 or 2) to extended columnar anions, that can be assumed to be present in the subsequent nucleation centres, might be expected to generate a family of structurally related phases $A_2[As_{2y}S_{3y+1}]$, whose postulated polyanions are depicted in Fig. 6. In contrast, the ability of Sb^{III} to participate in both ψ-SbS_3 tetrahedra and ψ-SbS_4 trigonal bipyramids leads to a fascinating diversity of the cation-directed connectivity patterns in the analogous thioantimonates(III). Although four- and six-membered Sb_2S_2 and Sb_3S_3 ring systems can frequently be recognised as characteristic molecular building blocks, any development of mechanistic guidelines is greatly hampered by the sheer diversity of potential structure types (*e.g.* Table 1 for $^1_\infty[Sb_4S_7]^{2-}$ polyanions) for this class of compounds. However, as the adoption of hypervalent co-ordination polyhedra by trivalent antimony can be assumed first to take place during the generation of the final solid state structure, the simpler thioarsenates(III) should also represent suitable mechanistic models for the initial condensation of pyramidal thioantimonate(III) anions in solution. Support for this assumption is provided by the presence of columnar substructures of the types depicted in Fig. 6 (M = Sb) in many of the known Sb_2S_3-based materials.

My group has been successful[19,70–73] in generating thioarsenates(III) $A_2[As_{2y}S_{3y+1}]$ for y = 1–4 (Table 2) by employing alkali metal or alkylammonium cations as structure-directing agents under mild solventothermal conditions (superheated water or CH_3CN). A relationship between the size of the counter cation A and the condensation grade c of the resulting polyanion (*e.g.* c = 0.50 for Na^+, c = 0.615 for Cs^+) is clearly apparent for the examples listed in Table 2. In analogy to the *zweier* $^1_\infty[AsS_2]^-$ chains of $RbAsS_2$[70] (Fig. 6a, alternative formulation $^1_\infty[As_2S_4]^{2-}$), corner-bridged ψ-$AsSe_3$ tetrahedra are present in the selenidoarsenate(III) chains of $AAsSe_2$ (A = K, Rb or Cs), that can likewise be isolated from a superheated methanol solution.[74] $RbSbS_2$ and $[Ba(en)_4][Sb_2Se_4]$ provide examples of analogous columnar chalcogenidoantimonates(III).[75,76] In contrast, the

Table 2 Alkali metal and alkylammonium thioarsenates(III) of the family $A_2[As_{2y}S_{3y+1}]$

Nuclearity $2y$	Dimensionality d	Examples A	References
2	1	Na[a]	69
	1	Rb	70
4	1	Me_4N	19
6	1	Me_4N	19
	1	Et_4N	71
8	1	$A(H_2O)$, A = K, Rb, NH_4	72
	1	Et_4N	71
	2	Cs	73

[a] Prepared by heating As_2S_3 in an Na_2S flux at 220 °C.

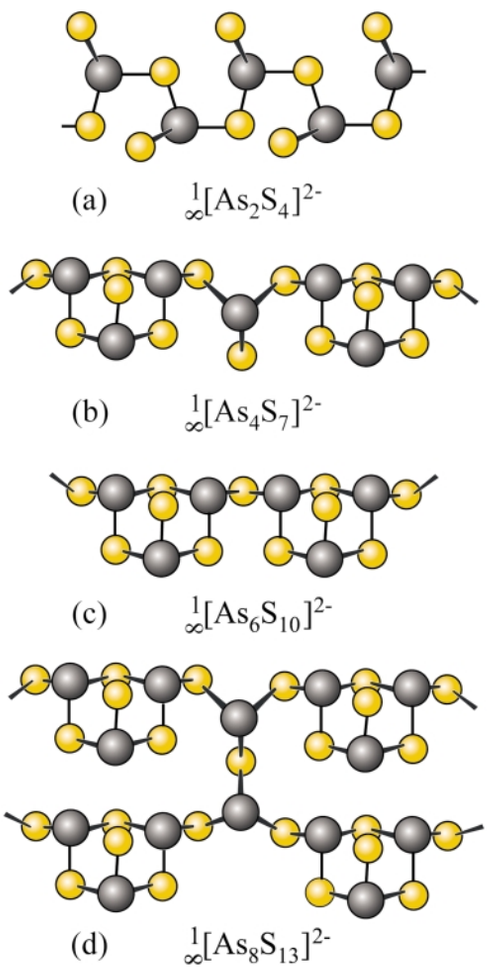

Fig. 6 Potential chain anions $^1_\infty[\{As_{2y}S_{3y+1}\}]^{2-}$, $y = 1$–4, resulting from the condensation of cyclic $As_3S_6^{3-}$ and linear $[As_yS_{2y+1}]^{(y+2)-}$ anions ($y = 1$ or 2).

trivalent antimony atoms extend their co-ordination number to 4 in the presence of the smaller NH_4^+ and K^+ cations of NH_4SbS_2[77] and $KSbS_2$,[78] whose $^1_\infty[SbS_2]^-$ chains contain a spiro-cyclic arrangement of four-membered Sb_2S_2 rings, similar to that in $Rb_2Sb_4S_7$[49] (Fig. 2b). This characteristic propensity of Sb(III) to participate in such ψ-SbE_4 trigonal bipyramids and the thereby resulting variety of possible repeat units is reflected in the frequent occurrence of $^1_\infty[\{Sb_yE_{2y}\}]^{y-}$ chains as sub-structures in Sb_2E_3-based materials.

Alternating corner bridging of $M_3S_6^{3-}$ and MS_3^{3-} anions generates the $^1_\infty[M_4S_7]^{2-}$ ribbons (Fig. 6b) of $(Me_4N)_2As_4S_7$[19] (Fig. 2a) and the thioantimonates(III) $(NH_4)_2Sb_4S_7$,[50] (H_2pip)-Sb_4S_7[51] and $[Mn(en)_3][Sb_4S_7]$,[52] in the latter two of which the presence of voluminous counter cations may well be instrumental in preventing ψ-SbS_4 trigonal bipyramids. However,

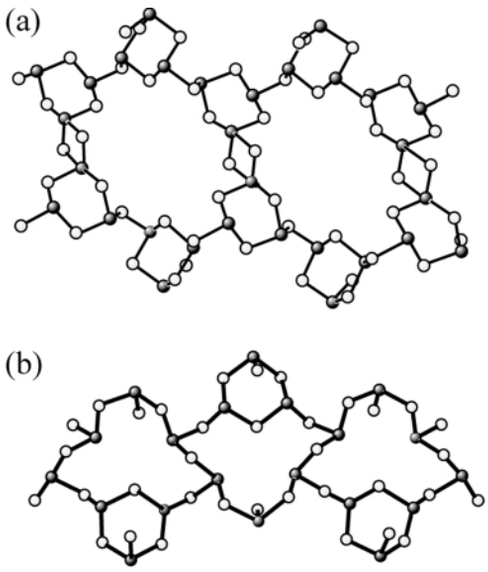

Fig. 7 $^1_\infty[As_6S_{10}]^{2-}$ chains in (a) $(Me_4N)_2As_6S_{10}$[19] and (b) $(Et_4N)_2$-As_6S_{10}.[71]

the possibility of participating in weak secondary M···S interactions does lead the free terminal S atoms of the $M_3S_6^{3-}$ building blocks to adopt unusual axial sites relative to their respective chair-shaped M_3S_3 rings. For instance, the relevant As···S distances in $(Me_4N)_2As_4S_7$ are 3.053(3) and 3.118(3) Å. On taking these contacts into account, M_3S_4 semicubes similar to those often found in lamellar thio- and selenido-stannates(IV) (Section 6) can be recognised as molecular building units.

Two $^1_\infty[Sb_4S_7]^{2-}$ chains interconnect through common Sb_2S_2 rings with four-co-ordinate antimony(III) atoms in $SrSb_4S_7 \cdot 6H_2O$.[54] Somewhat surprisingly, the postulated single chains of Fig. 6(c) are also joined through M_2S_2 rings in $(Me_4N)_2$-As_6S_{10}[19] (Fig. 7a), which represents the only known example of a thioarsenate(III) with relatively undistorted ψ-AsS_4 trigonal bipyramids. In contrast one half of the potential As_3S_3 rings in $(Et_4N)_2As_6S_{10}$[71] appear to have opened to provide the corner-bridging S atoms that link the component single chains of the polymeric anion (Fig. 7b). The practicability of extending these "Lego-like" building principles to the more highly condensed $^1_\infty[As_8S_{13}]^{2-}$ anions of Fig. 6(d), by choice of suitable structure-directing cations, has been confirmed by the recent preparation of $(Et_4N)_2As_8S_{13}$.[71] Corner bridging of cyclic $M_3S_6^{3-}$ and dipyramidal $M_2S_5^{2-}$ anions generates the double chains of the type $^1_\infty[M_8S_{13}]^{2-}$ found in $(Et_4N)_2As_8S_{13}$ (Fig. 8a), $A_2As_8S_{13} \cdot H_2O$ (A = K, Rb or NH_4) (Fig. 8b),[72] the mineral Gerstleyite $Na_2[(As, Sb)_8S_{13}] \cdot 2H_2O$[79] and $(H_2en)Sb_8S_{13}$.[80] Alternatively, this connectivity pattern may be regarded as resulting from the condensation of $^1_\infty[M_4S_7]^{2-}$ chains (Fig. 6b) of the type found in $(Me_4N)_2As_4S_7$[19] or $(NH_4)_2Sb_4S_7$.[50] The presence of such $^1_\infty[Sb_4S_7]^{2-}$ ribbons as a characteristic substructure in so many thioantimonates(III) is in accordance with a cation-directed prefabrication of medium-range columnar anions of this type prior to long-range structure generation. For instance, $^1_\infty[Sb_4S_7]^{2-}$ polyanions are linked through S–S bonds in the double chains of $(Me_2NH_2)_2Sb_8S_{14}$[81] and, when its Sb···S contacts longer than 3.0 Å are ignored, $[H_3N(CH_2)_3NH_3]Sb_{10}S_{16}$[82] also contains comparable $^1_\infty[Sb_{10}S_{16}]^{2-}$ double chains, in which corner-shared *cis*-$[Sb_2S_4]^{2-}$ units take over the bridging role.

In contrast to the more general structure-directing function of the counter cations in 1-D polyanions of the type $^1_\infty[M_4S_7]^{2-}$ or $^1_\infty[M_8S_{13}]^{2-}$, a specific templating role is apparent for the Cs^+ cations in the only known lamellar thioarsenate(III), Cs_2-As_8S_{13}.[73] As illustrated in Fig. 9, the alkali metal cations induce the formation of crown-shaped As_4S_4 rings (compare with

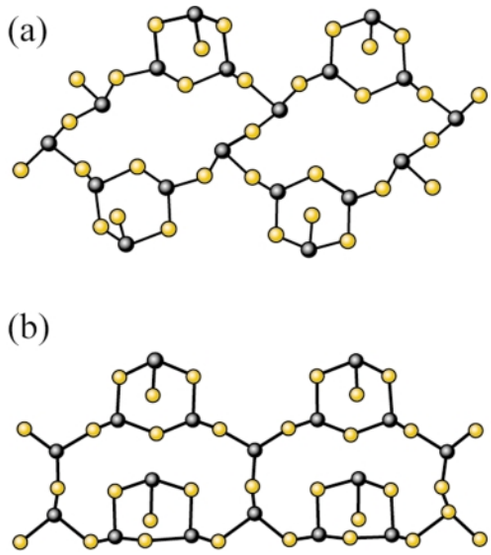

Fig. 8 $^{1}_{\infty}[As_8S_{13}]^{2-}$ chains in (a) $(Et_4N)_2As_8S_{13}$ [71] and (b) $A_2As_8S_{13}\cdot H_2O$ (A = K, Rb or NH_4).[72]

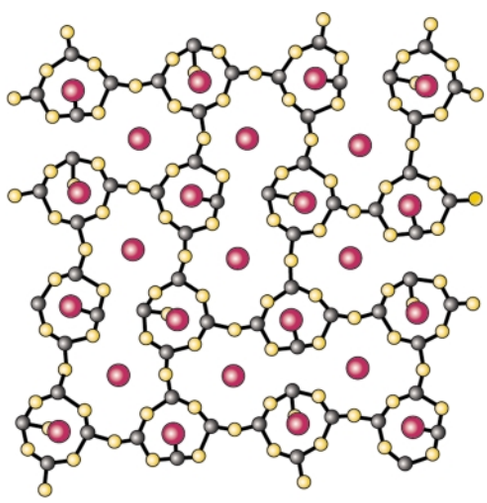

Fig. 9 The $^{2}_{\infty}[As_8S_{13}]^{2-}$ layers in $Cs_2As_8S_{13}$.[73]

Cs_4Te_{28} and Cs_3Te_{22} in Section 4) that are connected into infinite layers by As–S–As bridges.

The general principles of network construction discussed in this Section for ternary chalcogenido-arsenates(III) and -antimonates(III) can also be extended to Group 15 M_2E_3-based quaternary phases.[13] For instance infinite $^{1}_{\infty}[AsSe_2]^{-}$ chains can be recognised in the $^{2}_{\infty}[AgAs_3Se_6]^{2-}$ layers of $A_2AgAs_3Se_6$ (A = K or Rb)[83] and $As_3S_6^{3-}$ rings in the $^{2}_{\infty}[\{Bi(As_3S_6)_2\}]^{3-}$ sheets of $(Me_4N)_2Rb[Bi(As_3S_6)_2]$.[84]

6 Structure direction of thio- and selenido-stannates(IV)

The design of ternary thio- and selenido-germanates(IV) with open 2-D and 3-D anion networks is hampered by the ready participation of the predominant (pH < 11) adamantane-like $[Ge_4E_{10}]^{4-}$ anions in salt formation with a wide range of countercations (A = Na to Cs).[13] To my knowledge, only one chalcogenidogermanate(IV) sheet anion has structurally been characterised, namely $^{2}_{\infty}[Ge_2Se_5]^{2-}$ in $Na_2Ge_2Se_5$,[85] in which individual $GeSe_4$ tetrahedra are connected through three shared corners. However, quaternary thio- and selenido-germanates(IV) such as $[Me_4N]_2[MGe_4S_{10}]$ (M = Mn, Fe, Co or Cd)[86–88] and $A_3[AgGe_4Se_{10}]\cdot 2H_2O$ (A = Rb or Cs)[89] in which $[Ge_4E_{10}]^{4-}$ building units are linked through transition or coinage metals into zinc blende-like networks can readily be prepared under

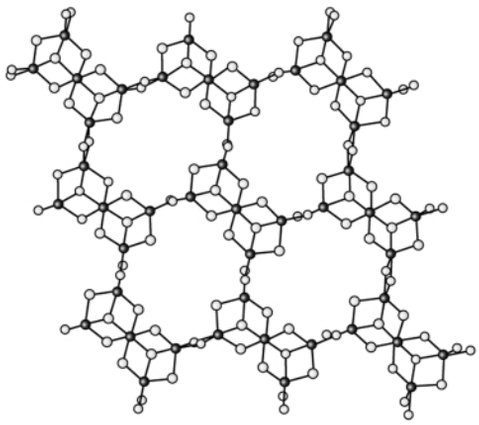

Fig. 10 The $^{2}_{\infty}[Sn_5S_{12}]^{4-}$ sheets in $Cs_4Sn_5S_{12}\cdot 2H_2O$.[34]

mild hydrothermal conditions. Mesoporous metal GeS_2-based materials have also recently been obtained in the presence of quaternary alkylammonium surfactants[90–92] and their potential employment as chemical sensors or for the detoxification of heavy metals in polluted water discussed.[90]

In contrast to the effective absence of ternary GeE_2-based materials, a rich variety of polymeric thio- and selenido-stannates(IV) are now known.[13] Following the initial reports of our group (1988–1993) on the solventothermal synthesis and structural characterisation of the prototypes $Cs_4Sn_5S_{12}\cdot 2H_2O$ (Fig. 10),[34] $Cs_2Sn_3Se_7$,[36] $(Me_2NH_2)_2Sn_3Se_7$ and $(H_2en)Sn_3Se_7\cdot 0.5en$,[93] interest in possible ion exchange, molecular recognition and optoelectronic applications of such lamellar chalcogenido-stannates(IV) has led to a spate of structural and physical studies on this class of compounds over the past five years.[94,95] The technological potential of microporous thiometalates of the heavier Group 14 elements Ge and Sn appears to have been discussed in depth for the first time in an article by Bedard *et al.* in 1989.[96] Recent employment of a range of alkylammonium counter ions to direct the construction of thiostannate(IV) sheets under mild hydrothermal conditions has underlined the influence of cation spatial requirements on the self-assembly process. As the counter ion size increases from that of $[Cs(H_2O)_2]^{+}$ in $Cs_4Sn_5S_{12}\cdot 2H_2O$ [34] over Me_4N^{+} and Et_4N^{+} in $(R_4N)_2Sn_3S_7\cdot xH_2O$ (R = Me, $x = 1$;[97] R = Et, $x = 0$ [3]) to that of nPr_4N^{+} or nBu_4N^{+} in $(R_4N)_2Sn_4S_9$,[98,99] so does the size of the cavities in the anionic networks from 20 to 24 and finally 32 members. This change in the degree of voidness is accompanied by a continuous increase in the anion condensation grade *c* (0.417, 0.429, 0.444) and a concomitant reduction in the average co-ordination number *n* of the tin atoms (5.33, 5.0, 4.75) in these thiostannates(IV). All three anionic networks of the series $^{2}_{\infty}[Sn_5S_{12}]^{4-}$ (Fig. 10), $^{2}_{\infty}[Sn_3S_7]^{2-}$ (see Fig. 13c for the analogous $^{2}_{\infty}[Sn_3Se_7]^{2-}$ sheets) and $^{2}_{\infty}[Sn_4S_9]^{2-}$ contain characteristic Sn_3S_4 "semicubes" in which the tin atoms of an Sn_3S_3 six-membered ring are bridged by a fourth sulfur atom. These molecular building blocks are joined into honeycomb nets in polyanions of the type $^{2}_{\infty}[Sn_3S_7]^{2-}$ through shared $(SnS)_2$ rings, in which the participating Sn atoms exhibit a trigonal bipyramidal co-ordination geometry. In the presence of very large structure-directing cations (*e.g.* nPr_4N^{+}, nBu_4N^{+}), edge-bridged Sn_6S_{10} double semicubes are linked through SnS_4 tetrahedra to provide the elongated 32-membered rings of the $^{2}_{\infty}[Sn_4S_9]^{2-}$ layers.

The generation of thio- and selenido-stannates(IV) $A_2Sn_3E_7$ by a wide range of structure-directing cations A^{+} (E = S, A = Me_4N,[97] Me_3NH,[100] NH_4, Et_4N, nPr_3NH, $tBuNH_3$,[3] or Hdabco;[101] E = Se, A = Cs [36] or Me_2NH_2 [93]) appears to be a consequence of the conformational flexibility of their component $^{2}_{\infty}[Sn_3E_7]^{2-}$ polyanions and of the ability of such sheets to adopt a variety of stacking arrangements. This latter phenomenon is reflected in the different space groups exhibited by members of this class of lamellar chalcogenidostannates(IV). *e.g.* (H_2en)-

Table 3 Alkali metal selenidostannates(IV) prepared in superheated solvents

Cation	*c*	*n*	*d*	Compound	Ref.
K^+	0.364	4	0	$K_6Sn_4Se_{11}\cdot 8H_2O$	39
	0.375	4	0	**$K_4Sn_3S_8$**[a]	41
	0.400	4	2	$K_4Sn_4Se_{10}\cdot 4.5H_2O$	107
Rb^+	0.333	4	0	**$Rb_4Sn_2Se_6$**	33
	0.364	4	0	$Rb_6Sn_4Se_{11}\cdot xH_2O$	39
	0.400	4	2	$Rb_4Sn_4Se_{10}\cdot 1.5H_2O$	107
	0.400	5	3	**$Rb_2Sn_2Se_5$**	42
	0.444	4.5	2	$Rb_2Sn_4Se_9\cdot H_2O$	35
Cs^+	0.333	4	0	**$Cs_4Sn_2Se_6$**	106
	0.400	4	1	$Cs_2Sn_2Se_5$	39
	0.400	4	1	$Cs_2Sn_2Se_5\cdot H_2O$	39
	0.400	4.5	2	$Cs_4Sn_4Se_{10}\cdot 3.2H_2O$	107
	0.429	5	2	**$Cs_2Sn_3Se_7$**	36
	0.444	4.5	2	$Cs_2Sn_4Se_9\cdot H_2O$	35

[a] Compounds prepared under methanolothermal conditions are given in bold type. All other phases were isolated from water–CH_3OH mixtures.

$Sn_3Se_7$0.5en, *Fddd*, $Cs_2Sn_3Se_7$, *C*2/*c*, $(Me_2NH_2)_2Sn_3Se_7$, $P2_1/n$. In accordance with the confirmed ability of $^2_\infty[Sn_3E_7]^{2-}$ layers to stack in the presence of a striking variety of counter cations is also the observation[97] that alkali and alkaline earth metal ions as well as some transition metal ions can replace the Me_4N^+ cations of $(Me_4N)_2Sn_3S_7\cdot H_2O$. Using real-time *in situ* energy-dispersive X-ray diffraction, O'Hare and co-workers[102] have reported that the construction of an ordered stacking arrangement for this thiostannate(IV) proceeds *via* a rapidly formed poorly crystalline layered material with disordered $^2_\infty[Sn_3S_7]^{2-}$ sheets. Their results indicate that whereas temperature is the primary factor in determining whether crystalline products are obtained, both pH and the nature of the chosen starting materials (*e.g.* SnS_2 or elemental Sn and S) can be of importance in controlling the rate of reaction and the generation of a particular polytype. Indeed Ozin and co-workers[101] have demonstrated that the $^2_\infty[Sn_3S_7]^{2-}$ layers of $(Hdabco)_2Sn_3S_7$ can, in fact, be constructed from an aqueous $Sn_2S_6^{4-}$ solution at room temperature by careful pH control.

The condensation mechanism of individual molecular building blocks required for the cation-directed construction of $^2_\infty[Sn_3S_7]^{2-}$ sheets has also been a matter of recent debate. For instance, Ozin, Bedard and co-workers have suggested[103–105] that the dominating ditetrahedral solution species $Sn_2S_6^{4-}$ could snap together in an initial step to create $Sn_4S_{11}^{6-}$ units that already contain the characteristic Sn_3S_4 semicubes. These building blocks can then assemble around the structure-directing cations to generate the $^2_\infty[Sn_3S_7]^{2-}$ sheets of porous thiostannates(IV). However, the adoption of a trigonal bipyramidal geometry by tin(IV) atoms in discrete tetranuclear units appears unlikely and $Sn_4S_{11}^{6-}$ anions of the above type have never been isolated.

Studies of my group on the solventothermal preparation of selenidostannates(IV) both in superheated CH_3OH and in CH_3OH–water mixtures now allow us to propose a very different reaction pathway to lamellar chalcogenidostannates(IV). In addition to the layered compounds of the type $A_2Sn_3Se_7$ (A = Cs or Me_2NH_2)[36,93] and BSn_3Se_7 (B = H_2en)[93] discussed previously, discrete edge-bridged di- and tri-tetrahedral anions in $Rb_4Sn_2Se_6$,[33] $Cs_4Sn_2Se_6$[106] and $K_4Sn_3Se_8$,[41] sheet anions $^2_\infty[Sn_2Se_6]^{2-}$ in $Cs_2Sn_2Se_6$[35] and the framework anion $^3_\infty[Sn_2Se_5]^{2-}$ of $Rb_2Sn_2Se_5$[42] can also be isolated under mild methanolothermal conditions. Performing reactions between the cation source and mineraliser A_2CO_3 (A = K, Rb or Cs), Sn and Se in superheated water/methanol reaction media favours the incorporation of water molecules into the co-ordination sphere of the structure-directing alkali metal ion leading, thereby, to such variations in the effective shape and size of the counter cation as are necessary to suit a particular anionic network. Under these conditions, careful pH control in the range 11–13 then enables the isolation of structurally related selenidostannates(IV) (Table 3) of the formula types $A_6Sn_4Se_{11}\cdot xH_2O$ (A = K or Rb),[39] $A_2Sn_2Se_5\cdot xH_2O$ (A = Cs),[39] $A_4Sn_4Se_{10}\cdot 3.2H_2O$ (A = Cs)[107] and $A_2Sn_4Se_9\cdot H_2O$ (A = Rb or Cs).[35] At a starting pH of 11.5–12.0 both yellow $Rb_6Sn_4Se_{11}\cdot xH_2O$ with its discrete $Sn_4Se_{11}^{6-}$ anions (Fig. 11b) and black $Rb_2Sn_4Se_9\cdot H_2O$ with its $^2_\infty[Sn_4Se_9]^{2-}$ sheets (Fig. 11d) can be prepared from a 1:2 water–CH_3OH reaction solution. Particularly interesting in this respect is the observation that the former phase can be crystallised from the remaining mother liquor at −8 °C following solventothermal generation of the latter lamellar selenidostannate(IV) at 115 °C. Under similar conditions, infinite $^1_\infty[Sn_2Se_5]^{2-}$ chains ($Cs_2Sn_2Se_5\cdot xH_2O$) and analogous $^2_\infty[Sn_4Se_9]^{2-}$ layers ($Cs_2Sn_4Se_9\cdot H_2O$) can simultaneously be isolated at 130 °C in the presence of the larger Cs^+ cation. The smaller K^+ cation, in contrast, generates only the tetranuclear $Sn_4Se_{11}^{6-}$ anion ($K_6Sn_4Se_{11}\cdot 8H_2O$), which consists of two corner-bridged ditetrahedral $Sn_2Se_6^{4-}$ units. These findings strongly suggest that both $Sn_4Se_{11}^{4-}$ and extended $^1_n[Sn_2Se_5]^{2-}$ columnar anions (Fig. 11c) must be regarded as precursors of the lamellar $^2_\infty[Sn_4Se_9]^{2-}$

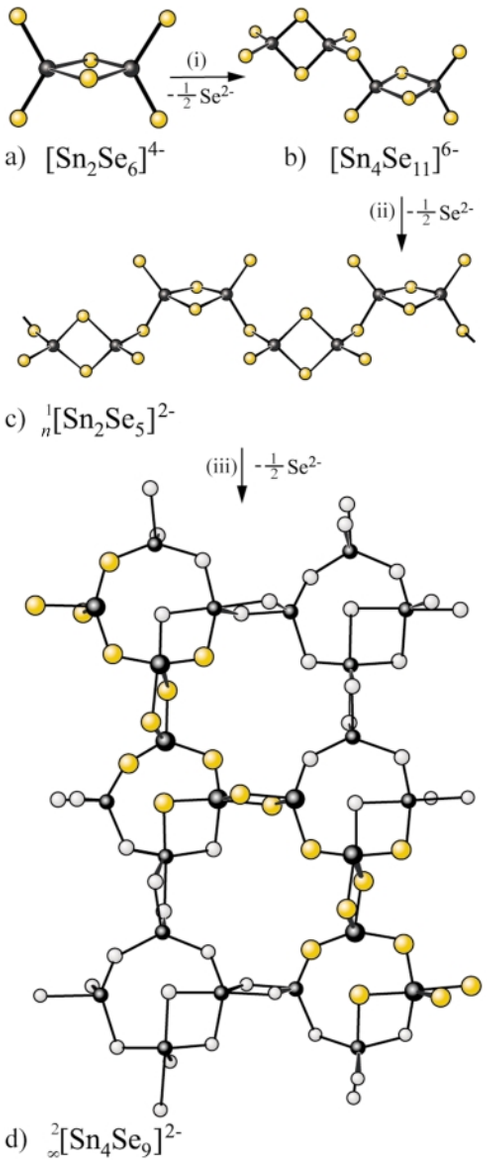

Fig. 11 Proposed reaction mechanism for the construction of $^2_\infty[Sn_4Se_9]^{2-}$ sheets from individual ditetrahedral $Sn_2Se_6^{4-}$ anions. A $^1_\infty[Sn_2Se_5]^{2-}$ chain is highlighted as a characteristic substructure of the $^2_\infty[Sn_4Se_9]^{2-}$ anions.

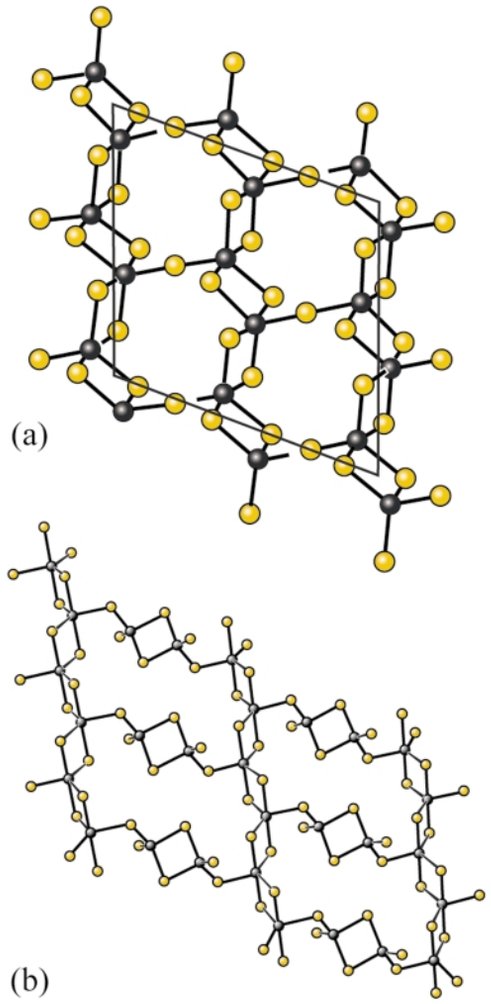

Fig. 12 Cross linking of $^{1}_{\infty}[SnSe_3]^{2-}$ ribbons (a) through common equatorial Se atoms in $Rb_2Sn_2Se_5$[42] and (b) through corner bridging with $Sn_2Se_6^{4-}$ anions in $Cs_4Sn_4Se_{10}\cdot 3.2H_2O$.[107]

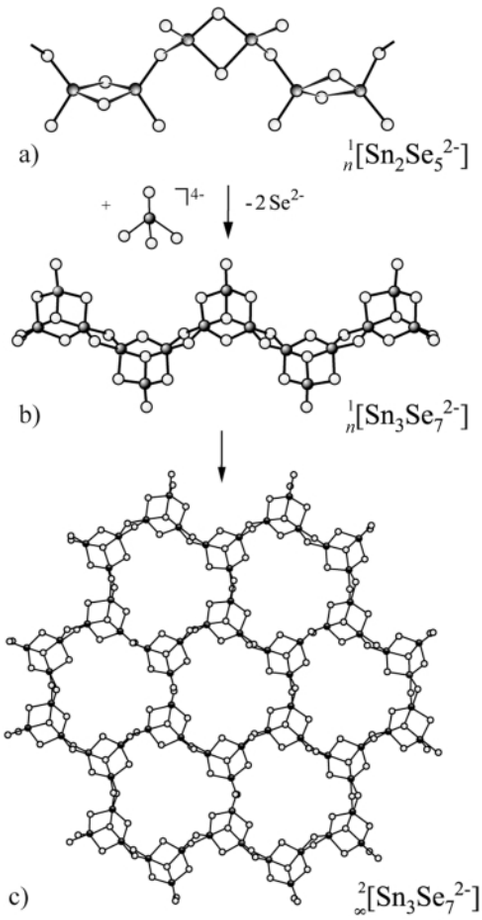

Fig. 13 Proposed reaction mechanism for the generation of lamellar $^{2}_{\infty}[Sn_3Se_7]^{2-}$ anions with their characteristic semicube units from $^{1}_{n}[Sn_2Se_5]^{2-}$ chains.

anions and allow us to propose the condensation steps summarised in Fig. 11 as representing the probable mechanistic route to the final sheet structure from the predominant ditetrahedral solution species $Sn_2Se_6^{4-}$.

Many of the known 2- and 3-dimensional chalcogenidostannates(IV) exhibit $^{1}_{\infty}[SnE_3]^{2-}$ chains with edge-bridged component SnE_5 trigonal bipyramids, as a characteristic structural motif. Such ribbons are themselves unknown as polyanions but could result from a nucleophilic attack of E^{2-} on adjacent tin atoms of $^{1}_{\infty}[Sn_2E_5]^{2-}$ chains of the type depicted in Fig. 11(c). Condensation of $^{1}_{\infty}[SnSe_3]^{2-}$ ribbons through shared terminal Se atoms would afford the framework $^{3}_{\infty}[Sn_2Se_5]^{2-}$ networks of $Rb_2Sn_2Se_5$ (Fig. 12a); formation of direct Se–Se bonds between parallel $^{1}_{\infty}[SnSe_3]^{2-}$ chains would generate the $^{2}_{\infty}[Sn_2Se_6]^{2-}$ sheets of $Cs_2Sn_2Se_6$.[35] It is, of course, quite possible that the increase in the tin co-ordination number from 4 to 5, leading to formation of the characteristic $^{1}_{\infty}[SnSe_3]^{2-}$ columns with an associated increase in phase density, will first take place after connection of the $^{1}_{\infty}[Sn_2Se_5]^{2-}$ ribbons through shared terminal Se atoms or Se–Se bonds. A further structurally related example is provided by $Cs_4Sn_4Se_{10}\cdot 3.2H_2O$, which can be prepared at high pH (12.0–13.0). Ditetrahedral $Sn_2Se_6^{4-}$ anions are employed as spacer units to link the $^{1}_{\infty}[SnSe_3]^{2-}$ columns in this case (Fig. 12b).

My group has also recently been successful in isolating a possible "missing link" on the reaction pathway from $Sn_2Se_6^{4-}$ to honeycomb $^{2}_{\infty}[Sn_3Se_7]^{2-}$ sheets (Fig. 13c) with their characteristic Sn_3Se_4 semicubes. $(Et_4N)_2Sn_3Se_7$ can be prepared under mild methanolothermal conditions[39] and contains *zweier* $^{1}_{\infty}[Sn_3Se_7]^{2-}$ chains (Fig. 13b), whose component semicube Sn_3Se_7 building units are connected through common edges. As illustrated in Fig. 13, after condensation of $^{1}_{\infty}[Sn_2Se_5]^{2-}$ chains with tetrahedral $SnSe_4^{4-}$ anions, a concerted nucleophilic attack of the terminal Se atoms on the tetrahedral Sn atoms of adjacent $^{1}_{\infty}[Sn_3Se_7]^{2-}$ ribbons would generate the typical 6^3 net of $^{2}_{\infty}[Sn_3Se_7]^{2-}$. Alternatively such lamellar selenidostannates(IV) could result from a direct condensation of $^{1}_{\infty}[Sn_2Se_5]^{2-}$ chains through individual bridging ditetrahedral $Sn_2Se_6^{4-}$ species. Indeed the $^{2}_{\infty}[Sn_4Se_{10}^{4-}]$ sheets of $Cs_4Sn_4Se_{10}\cdot 3.2H_2O$ (Fig. 12b) can be regarded as representing just such a possible intermediate structure (albeit with twice the number of bridging $Sn_2Se_6^{4-}$ units) between the $^{1}_{\infty}[Sn_2Se_5]^{2-}$ chains of $Cs_2Sn_2Se_5\cdot xH_2O$ and the $^{2}_{\infty}[Sn_3Se_7]^{2-}$ nets of $Cs_2Sn_3Se_7$, that can be isolated with the same counter cation (without additional water ligands) from superheated methanol. It is apparent that characteristic Sn_3Se_4 semicubes need only be constructed in the final stages of either of the suggested mechanisms for network assembly. Our proposal that extended $^{1}_{n}[Sn_2E_5]^{2-}$ columnar anions play a central role in the cation-directed generation of SnE_2-based networks can readily be extended to thiostannates(IV) (*e.g.* $A_2Sn_3S_7$, $A_2Sn_4S_9$). However, the ability of Sn^{IV} to exhibit a co-ordination number of 6 in such materials also allows the adoption of network topologies not possible for the selenidostannates(IV). For instance, whereas individual $^{1}_{\infty}[SnS_3]^{2-}$ chains in $Cs_4Sn_5S_{12}\cdot 2H_2O$[34] are linked by edge-bridged SnS_6 octahedra, two such substructures condense in $A_2Sn_3S_7\cdot xH_2O$ (A = K or Rb)[33] to bioctahedral rods, that can themselves be regarded as fragments of the close-packed SnS_2 structure. Ditetrahedral $Sn_2S_6^{4-}$ units join these double chains into a disordered sheet. It is also interesting that, in contrast to $(Et_4N)_2Sn_3Se_7$, the analogous thiostannate(IV) contains $^{1}_{\infty}[Sn_3S_7]^{2-}$ honeycomb layers.[3] This observation provides supporting evidence for our proposed

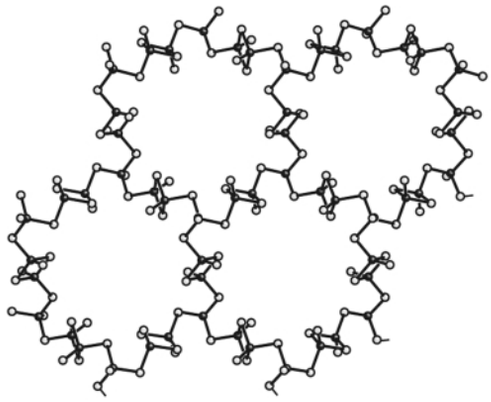

Fig. 14 The open 6^3 net of the $^2_\infty[Sn_4Se_{10}]^{4-}$ anions in $K_4Sn_4Se_{10}\cdot 4.5H_2O$ and $Rb_4Sn_4Se_{10}\cdot 1.5H_2O$.[107]

reaction pathway and underlines that fine-tuning of space-filling factors can be of critical importance in determining which particular anionic network will be self-assembled under mild solventothermal conditions.

A contrasting mechanism is required to explain the formation of the very open 6^3 nets of $K_4Sn_4Se_{10}\cdot 4.5H_2O$ and $Rb_4Sn_4Se_{10}\cdot 1.5H_2O$[107] that can be prepared at very high pH values (12.0–13.0). The ratio of mononuclear $SnSe_4^{4-}$ anions to ditetrahedral $Sn_2Se_6^{4-}$ species will increase as the pH rises leading thereby to the incorporation of corner-bridged $SnSe_4^{4-}$ tetrahedra as a second building block in these unique $^2_\infty[Sn_4Se_{10}]^{4-}$ sheet anions (Fig. 14) with their remarkable nanometer-sized (12.9 × 14.1 Å) 36-membered cavities.

7 Summary and outlook

The original motivation for my group's detailed investigation of parameter influence (*e.g.* temperature, cation size and shape, pH , solvent polarity) on solventothermal reaction pathways to Main Group chalcogenidometalates was stimulated by the goal of developing a rational approach to synthetic strategies for this promising class of materials. As reviewed in this article, the presence of predominant solution species such as cyclic trigonal pyramidal $M_3S_6^{3-}$ (M = As or Sb) or ditetrahedral $Sn_2E_6^{4-}$ anions (E = S or Se) as molecular building units and their participation in columnar substructures (*e.g.* $^1_\infty[M_4S_7]^{2-}$, $^1_\infty[SnE_3]^{2-}$) is characteristic for thio- and selenido-metalates of As, Sb and Sn. Topological relationships between individual members of structural families of the type $A_xM_yE_z$ with a steadily increasing degree of anion condensation *c* provide a detailed insight into probable cation-directed self-assembly mechanisms. This, in its turn, enables the development of guidelines for the employment of alkali metal or alkylammonium ions in controlling the condensation of small solution species into chains, sheets or frameworks, whose channels or cavities reflect the spatial requirements of the structure-directing agent. Examples for the feasibility of this approach are provided by columnar thioarsenates(III) of the type $A_2[As_{2y}S_{3y+1}]$, $y = 1$–4, lamellar thiostannates(IV) of the series $A_4Sn_5S_{12}$, $A_2Sn_3S_7$ and $A_2Sn_4S_9$, and alkali metal selenidostannates(IV) of the structural family $A_6Sn_4Se_{11}$, $A_2Sn_2Se_5$ and $A_2Sn_4Se_9$ (as hydrates). The extension of such guidelines to potentially multifunctional quaternary phases or composite materials with metal chalcogenide-based substructures (*e.g.* defective square-planar tellurium nets or $^1_\infty[SnE_3]^{2-}$ chains) presents an exciting current synthetic challenge.

Acknowledgements

I would particularly like to thank all my past and present Ph.D. students who have so enthusiastically contributed to our own research efforts in this area. These are in chronological order: Jürgen Kaub, Hans-Joachim Häusler, Hans Georg Braunbeck, Bernhard Schaaf, Michael Wachhold, Anja Loose and Viola Vater. Support by the Fonds der Chemischen Industrie and the Deutsche Forschungsgemeinschaft is also gratefully acknowledged.

References

1 C. L. Bowes and G. A. Ozin, *Adv. Mater.*, 1996, **8**, 13.
2 A. K. Cheetham, G. Férey and T. Loiseau, *Angew. Chem., Int. Ed. Engl.*, 1999, **38**, 3269.
3 H. Ahari, C. L. Bowes, T. Jiang, A. Lough, G. A. Ozin, R. L. Bedard, S. Petrov and D. Young, *Adv. Mater.*, 1995, **7**, 375.
4 T. Jiang, G. A. Ozin, A. Verma and R. L. Bedard, *J. Mater. Chem.*, 1998, **8**, 1649.
5 W. S. Sheldrick, M. Wachhold, S. Jobic, R. Brec and E. Canadell, *Adv. Mater.*, 1997, **9**, 669.
6 M. E. Davis and R. F. Lobo, *Chem. Mater.*, 1992, **4**, 756.
7 W. S. Sheldrick and M. Wachhold, *Angew. Chem., Int. Ed. Engl.*, 1997, **36**, 206.
8 J. Li, Z. Chen, R.-J. Wang and D. M. Proserpio, *Coord. Chem. Rev.*, 1999, **190**, 707.
9 R. J. Francis and D. O'Hare, *J. Chem. Soc., Dalton Trans.*, 1998, 3133.
10 C. T. G. Knight, R. T. Syvitski and S. D. Kinrade, *Stud. Surf. Sci. Catal.*, 1995, **97**, 483.
11 S. Oliver, A. Kuperman, A. Lough and G. A. Ozin, *Chem. Mater.*, 1996, **8**, 2391.
12 S. Oliver, A. Kuperman and G. A. Ozin, *Angew. Chem., Int. Ed.*, 1998, **37**, 46.
13 W. S. Sheldrick and M. Wachhold, *Coord. Chem. Rev.*, 1998, **176**, 211.
14 M. G. Kanatzidis, *Chem. Mater.*, 1990, **2**, 353.
15 M. G. Kanatzidis and A. C. Sutorik, *Prog. Inorg. Chem.*, 1995, **43**, 151.
16 D. Fenske, G. Kräuter and K. Dehnicke, *Angew. Chem., Int. Ed. Engl.*, 1990, **29**, 390.
17 M. G. Kanatzidis and S.-P. Huang, *Inorg. Chem.*, 1989, **28**, 4667.
18 B. Krebs, E. Lührs, R. Willmer and F.-P. Ahlers, *Z. Anorg. Allg. Chem.*, 1991, **592**, 17.
19 V. Vater and W. S. Sheldrick, *Z. Naturforsch., Teil B*, 1997, **52**, 1119.
20 G. P. Voutsas, A. G. Papazoglou, P. J. Rentzeperis and D. Siapkas, *Z. Kristallogr.*, 1985, **171**, 261.
21 G. Dittmar and H. Schäfer, *Z. Naturforsch., Teil B*, 1977, **32**, 1346.
22 W. S. Sheldrick and H.-J. Häusler, *Z. Anorg. Allg. Chem.*, 1988, **557**, 98.
23 G. Cordier and H. Schäfer, *Z. Naturforsch., Teil B*, 1979, **34**, 1053.
24 W. S. Sheldrick and J. Kaub, *Z. Anorg. Allg. Chem.*, 1986, **536**, 114.
25 L. Pauling, *J. Am. Chem. Soc.*, 1947, **69**, 542.
26 I. D. Brown and D. Altermatt, *Acta Crystallogr., Sect. B*, 1985, **41**, 244.
27 M. O' Keeffe and N. E. Brese, *Acta Crystallogr., Sect. B*, 1992, **48**, 152.
28 W. S. Sheldrick and C. Horn, *Z. Naturforsch., Teil B*, 1989, **44**, 405.
29 X. Wang and F. Liebau, *Acta Crystallogr., Sect. B*, 1996, **52**, 7.
30 X. Wang and F. Liebau, *Z. Kristallogr.*, 1996, **211**, 437.
31 G. Cordier, H. Schäfer and C. Schwidetzky, *Rev. Chim. Miner.*, 1985, **22**, 676.
32 R. Cook and H. Schäfer, *Stud. Inorg. Chem.*, 1983, **3**, 757.
33 W. S. Sheldrick and B. Schaaf, *Z. Anorg. Allg. Chem.*, 1994, **620**, 1041.
34 W. S. Sheldrick, *Z. Anorg. Allg. Chem.*, 1988, **562**, 23.
35 A. Loose and W. S. Sheldrick, *Z. Naturforsch., Teil B*, 1998, **53**, 349.
36 W. S. Sheldrick and H. G. Braunbeck, *Z. Naturforsch., Teil B*, 1990, **45**, 1643.
37 W. S. Sheldrick and B. Schaaf, *Z. Naturforsch., Teil B*, 1994, **49**, 57.
38 F. Liebau, *Structural Chemistry of Silicates, Structure, Bonding and Classification*, Springer Verlag, Heidelberg, 1985.
39 A. Loose and W. S. Sheldrick, *Z. Anorg. Allg. Chem.*, 1999, **625**, 233.
40 W. S. Sheldrick, in *Structural Chemistry of Organic Silicon Compounds*, eds. S. Patai and Z. Rappoport, John Wiley & Sons, New York, 1989, p. 227.
41 W. S. Sheldrick, *Z. Naturforsch., Teil B*, 1988, **43**, 249.
42 W. S. Sheldrick and H. G. Braunbeck, *Z. Naturforsch., Teil B*, 1992, **47**, 151.
43 K. Volk and H. Schäfer, *Z. Naturforsch., Teil B*, 1979, **34**, 1637.
44 A. S. Kanishcheva, V. G. Kuznetzov, Y. N. Mikhailov, V. N. Batog and V. M. Skorikov, *Zh. Strukt. Khim.*, 1980, **21**, 136.
45 H. A. Graf and H. Schäfer, *Z. Naturforsch., Teil B*, 1972, **27**, 735.

46 W. Bensch and M. Schur, *Eur. J. Solid State Inorg. Chem.*, 1997, **34**, 457.
47 B. Eisenmann and H. Schäfer, *Z. Naturforsch.*, *Teil B*, 1979, **34**, 383.
48 G. Dittmar and H. Schäfer, *Z. Anorg. Allg. Chem.*, 1978, **441**, 93.
49 W. S. Sheldrick and H.-J. Häusler, *Z. Anorg. Allg. Chem.*, 1988, **557**, 105.
50 G. Dittmar and H. Schäfer, *Z. Anorg. Allg. Chem.*, 1977, **437**, 183.
51 J. B. Parise and Y. Ko, *Chem. Mater.*, 1992, **4**, 1446.
52 W. Bensch and M. Schur, *Z. Naturforsch.*, *Teil B*, 1997, **52**, 405.
53 G. Dittmar and H. Schäfer, *Z. Anorg. Allg. Chem.*, 1978, **441**, 98.
54 G. Cordier, H. Schäfer and C. Schwidetzky, *Z. Naturforsch.*, *Teil B*, 1984, **39**, 131.
55 P. Böttcher, *Angew. Chem.*, *Int. Ed. Engl.*, 1988, **27**, 759.
56 W. S. Sheldrick and M. Wachhold, *Angew. Chem.*, *Int. Ed. Engl.*, 1995, **34**, 450.
57 W. S. Sheldrick and B. Schaaf, *Z. Naturforsch.*, *Teil B*, 1994, **49**, 993.
58 M. Björgvinsson and G. J. Schrobilgen, *Inorg. Chem.*, 1991, **30**, 2540.
59 M. Björgvinsson, J. F. Sawyer and G. J. Schrobilgen, *Inorg. Chem.*, 1991, **30**, 4238.
60 L. D. Schultz and W. H. Koehler, *Inorg. Chem.*, 1987, **26**, 1989.
61 L. D. Schultz, *Inorg. Chim. Acta*, 1990, **176**, 271.
62 M. Wachhold and W. S. Sheldrick, *Z. Naturforsch.*, *Teil B*, 1996, **51**, 1235.
63 W. S. Sheldrick and M. Wachhold, *Chem. Commun.*, 1996, 607.
64 Q. Liu, N. Goldberg and R. Hoffmann, *Chem. Eur. J.*, 1996, **2**, 390.
65 S. Jobic, W. S. Sheldrick, E. Canadell and R. Brec, *Bull. Soc. Chim. Fr.*, 1996, **133**, 221.
66 E. Canadell, S. Jobic, R. Brec, J. Rouxel and M.-H. Whangbo, *J. Solid State Chem.*, 1992, **99**, 189.
67 S. V. Vorob'eva, A. A. Ivakin, A. M. Gorelov and E. M. Gertman, *Russ. J. Inorg. Chem.*, 1977, **22**, 1479.
68 W. S. Sheldrick and J. Kaub, *Z. Naturforsch.*, *Teil B*, 1985, **40**, 19.
69 M. Palazzi and S. Jaulmes, *Acta Crystallogr.*, *Sect. B*, 1977, **33**, 908.
70 H.-J. Häusler, Dissertation, Kaiserslautern, 1986.
71 V. Vater and W. S. Sheldrick, *Z. Naturforsch.*, *Teil B*, 1998, **53**, 1259.
72 W. S. Sheldrick and J. Kaub, *Z. Naturforsch.*, *Teil B*, 1985, **40**, 1130.
73 W. S. Sheldrick and J. Kaub, *Z. Naturforsch.*, *Teil B*, 1985, **40**, 571.
74 W. S. Sheldrick and H.-J. Häusler, *Z. Anorg. Allg. Chem.*, 1988, **561**, 139.
75 A. S. Kanishcheva, V. G. Kuznetsov, V. B. Lazarev and T. G. Tarsova, *Zh. Strukt. Khim.*, 1977, **18**, 1069.
76 T. König, B. Eisenmann and H. Schäfer, *Z. Anorg. Allg. Chem.*, 1982, **488**, 126.
77 A. K. Volk, P. Bickert, R. Kolmer and H. Schäfer, *Z. Naturforsch.*, *Teil B*, 1979, **34**, 380.
78 H. A. Graf and H. Schäfer, *Z. Anorg. Allg. Chem.*, 1975, **414**, 211.
79 I. Nakai and D. E. Appleman, *Chem. Lett.*, 1981, 1327.
80 K. Tan, Y. Ko and J. B. Parise, *Acta Crystallogr.*, *Sect. C*, 1994, **50**, 1439.
81 K. Tan, Y. Ko, J. B. Parise, J.-H. Park and A. Darovsky, *Chem. Mater.*, 1996, **8**, 2510.
82 X. Wang, *Eur. J. Solid State Inorg. Chem.*, 1995, **32**, 303.
83 M. Wachhold and M. G. Kanatzidis, *Inorg. Chem.*, 1999, **38**, 3863.
84 J.-H. Chou and M. G. Kanatzidis, *Inorg. Chem.*, 1994, **33**, 1001.
85 B. Eisenmann, J. Hansa and H. Schäfer, *Rev. Chim. Miner.*, 1984, **21**, 817.
86 O. M. Yaghi, Z. Sun, D. A. Richardson and T. L. Groy, *J. Am. Chem. Soc.*, 1994, **116**, 807.
87 O. Achak, J. Y. Pivan, M. Maunaye and M. Louër, *J. Alloys Compd.*, 1995, **219**, 111.
88 C. L. Bowes, A. J. Lough, A. Malek, G. A. Ozin, S. Petrov and D. Young, *Chem. Ber.*, 1996, **129**, 283.
89 A. Loose and W. S. Sheldrick, *Z. Naturforsch.*, *Teil B*, 1997, **52**, 687.
90 M. J. MacLachlan, N. Coombs and G. A. Ozin, *Nature* (*London*), 1999, **397**, 681.
91 M. J. MacLachlan, N. Coombs, R. L. Bedard, S. White, L. K. Thompson and G. A. Ozin, *J. Am. Chem. Soc.*, 1999, **121**, 12005.
92 M. Wachhold, K. K. Rangan, S. J. L. Billinge, V. Petkov, J. Heising and M. G. Kanatzidis, *Adv. Mater.*, 2000, **12**, 85.
93 W. S. Sheldrick and H. G. Braunbeck, *Z. Anorg. Allg. Chem.*, 1993, **619**, 1300.
94 T. Jiang and G. A. Ozin, *J. Mater. Chem.*, 1998, **8**, 1099.
95 R. W. J. Scott, M. J. MacLachlan and G. A. Ozin, *Curr. Opinion Solid State Mater. Res.*, 1999, **4**, 113.
96 R. L. Bedard, S. T. Wilson, L. D. Vail, J. M. Bennett and E. M. Flanigen, in *Zeolites, Facts, Figures, Future*, eds. P. A. Jacobs and R. A. van Santen, Elsevier, Amsterdam, 1989, p. 375.
97 J. B. Parise, Y. Ko, J. Rijssenbeck, D. M. Nellis, K. Tan and S. Koch, *J. Chem. Soc.*, *Chem. Commun.*, 1994, 527.
98 T. Jiang, A. J. Lough, G. A. Ozin and D. Young, *Chem. Mater.*, 1995, **7**, 245.
99 Y. Ko, C. L. Cahill and J. B. Parise, *J. Chem. Soc.*, *Chem. Commun.*, 1994, 69.
100 Y. Ko, K. Tan and J. B. Parise, *Acta Crystallogr.*, *Sect. C*, 1995, **51**, 398.
101 T. Jiang, A. Lough and G. A. Ozin, *Adv. Mater.*, 1998, **10**, 42.
102 R. J. Francis, S. J. Prince, J. S. O. Evans, S. O'Brian, D. O'Hare and S. M. Clark, *Chem. Mater.*, 1996, **8**, 2102.
103 T. Jiang, A. Lough, G. A. Ozin and R. L. Bedard, *J. Mater. Chem.*, 1998, **8**, 733.
104 T. Jiang, R. L. Bedard and G. A. Ozin, *Adv. Mater.*, 1995, **7**, 166.
105 Ö. Dag, H. Ahari, N. Coombs, T. Jiang, P. P. Aroca-Ouellette, S. Petrov, I. Sokolov, A. Verma, G. Vovk, D. Young, G. A. Ozin, C. Reber, Y. Pelletier and R. L. Bedard, *Adv. Mater.*, 1997, **9**, 1133.
106 W. S. Sheldrick and H. G. Braunbeck, *Z. Naturforsch.*, *Teil B*, 1989, **44**, 851.
107 A. Loose and W. S. Sheldrick, *J. Solid State Chem.*, 1999, **147**, 146.